JOURNAL OF COMPUTATIONAL PHYSICS 3, 273–290 (1968)

The Calculation of Steady Plane Supersonic Gas Flows Containing an Arbitrarily Large Number of Shocks*

DAVID B. TAYLOR

Argonne National Laboratory, Argonne, Illinois 60439

Received March 25, 1968

ABSTRACT

A scheme of computation is described which will allow the calculation of plane supersonic gas flow through ducts and around obstacles with an accuracy dependent mainly on the adequacy of the assumption that viscous and heat conductive effects may be confined to oblique shocks, these being represented by abrupt changes in flow variables. The computing scheme will keep track of an arbitrarily large number of discontinuities and will introduce those shocks, vortex sheets and midflow expansions which are necessary to represent discontinuity interactions. The methods used are applicable to the calculation of weak solutions of other hyperbolic systems.

1. INTRODUCTION

The computation of supersonic gas flows is impeded in many flows of interest by the presence of regions, known as shocks and vortex sheets, in which flow variables change very rapidly in an otherwise slowly varying flow field. If a large number of shocks and vortex sheets are of concurrent interest, a shock smearing technique requiring several grid points to represent each shock or vortex sheet will lead to a method having a very large number of grid points. Such methods have, of course, proved very useful in the study of transonic, shock, and boundary layer phenomena. Here, however, the emphasis lies in determining quickly and accurately supersonic gas flows in which shocks and vortex sheets interact as predicted by the Rankine Hugoniot equations and the isentropic flow relations. In fulfilling these aims, a general technique which determines weak solutions of hyperbolic systems in two space variables has been developed.

The weak solutions selected here for the gas flow equations are those which contain weak oblique shocks. The solutions may also contain vortex sheets and

---

* Work performed under the auspices of the United States Atomic Energy Commission.

discontinuities of derivatives of the flow variables on Mach lines and streamlines. The method given will produce accurate solutions of the selected class in the region in which the equations are hyperbolic. The utility of the solutions as descriptions of actual gas flow, particularly for marginally supersonic flows, must be assesed by considering the stability of the boundary layers necessary to sustain the computed flow and by examining the adequacy of the hypothesis that no Mach reflections or strong shocks occur.

The numerical techniques which have been employed are well known. The method of characteristics used by Hartree [1] to determine the solution on a family of space-like curves requires adaption to allow the fitting of shocks and vortex sheets into the flow. The method of linearization of nonlinear difference equations and of iterative solution by successive replacement which is used by Hartree is inadequate where the functions vary rapidly and special techniques have been devised to avoid nonconvergent or very slowly convergent algorithms. These are discussed in Section 4.

Shock fitting applied to one-dimensional time dependent flows are extensively discussed by Zhukov [2]. Moe and Troesch [3] have developed a shock fitting technique for two-dimensional steady flows. These methods operate in the context of a mesh of characteristic lines and some of the advantages are lost when a more general grid is used. An alternative scheme is described in Section 4.

The possibility of rotational flow requires that entropy be computed as part of the solution procedure. Powers [4] has shown how this may be done accurately using a stream function calculation. His technique is implicit in that used here.

The manipulation and control of intersections of generated discontinuities constituted the major programming task. The use of the normals to the streamlines of the flow as a basis for the manipulation is novel. The use of selected Mach lines to demarcate expansions and compressions and to maintain accuracy in the neighborhood of focus points is of course derived from the basic method of characteristics (see [3]). The retention of selected streamlines to maintain accuracy when the entropy gradient along normals is high is a natural extension of this approach. These features are combined to yield a method which will represent accurately, with a minimum of data, functions which are discontinuous and which may contain discontinuities of derivative or short intervals in which derivatives are relatively high.

The methods developed have been applied to flow in a duct. A specification of the flow at the inlet or upstream end of the duct provides primary boundary conditions. In order to provide the designer of supersonic intakes and nozzles with an adaptable computing tool, a variety of secondary boundary conditions have been implemented. The boundary streamlines—the walls of a duct—may be specified by their position, by defining the values of some fluid dynamic variable on them or by requiring that they produce a Mach line focus at a specified point.

A complete description of the method will appear in Ref. [5] in which the method is also applied to axisymmetric flows. Its salient features for plane flow will be given here.

2. The Choice of Space Coordinates

There are numerous advantages to be gained from use of a coordinate system based on measures along streamlines and along normals to streamlines. The boundary conditions are easily implemented and, since the normals are always spacelike, they are acceptable as a family on which to determine the solution using the Hartree variant of the method of characteristics. Mach line and shock manipulations are most readily carried out with this frame of reference and the need to discard parts of a calculated flow field because of the development of shocks is eliminated.

The equations to be solved, in characteristic form, are

$$\rho q \frac{\partial q}{\partial s} + \frac{\partial p}{\partial s} = 0, \tag{1}$$

$$\pm\rho q^2 \left(\frac{\partial \theta}{\partial s} \pm \frac{1}{(M^2-1)^{1/2}} \frac{\partial \theta}{\partial n}\right) + (M^2-1)^{1/2} \left(\frac{\partial p}{\partial s} \pm \frac{1}{(M^2-1)^{1/2}} \frac{\partial p}{\partial n}\right) = 0, \tag{2}$$

$$p/\rho^\gamma = K(n), \tag{3}$$

$$\left.\begin{aligned} x &= x_0 + \int_{s_0}^{s} \cos\theta \, ds \\ y &= y_0 + \int_{s_0}^{s} \sin\theta \, ds \end{aligned}\right\}, \tag{4}$$

where s is distance along a streamline; n is distance along a normal to the streamlines; p is pressure; ρ is density; q is velocity; θ is the inclination of a streamline to the x-axis; γ is the ratio of specific heats; M is the Mach number, $M^2 = \rho q^2/\gamma p$; $K(n)$ is a function determining the entropy on different streamlines; x and y are cartesian coordinates.

The perfect gas law, $p = \rho RT$, where R is a gas constant and T the temperature, should also be considered part of the system. Using this gas law in conjunction with Eq. (3), Eq. (1) can be integrated to give Bernoulli's equation,

$$\frac{1}{2} q^2 + \frac{\gamma p}{(\gamma - 1)\rho} = c_p T_0 ,$$

where c_p is the specific heat at constant pressure and T_0 is the stagnation temperature. In the procedure developed, (1) is solved numerically and (5) used to check the accuracy of the evaluation. This gives a measure of the accumulation of numerical error.

The distances s and n are inconvenient measures with which to define streamlines and normals to streamlines. The stream function defined by

$$\frac{\partial \psi}{\partial n} = \rho q, \qquad \frac{\partial \psi}{\partial s} = 0 \tag{6}$$

is constant on each streamline and may be used in place of n. In irrotational flow, a velocity potential ϕ satisfying

$$\frac{\partial \phi}{\partial s} = q, \qquad \frac{\partial \phi}{\partial n} = 0 \tag{7}$$

remains constant on normals. In rotational flow a suitable ϕ can be found if there exists a function $Q(s, n)$ such that

$$\frac{\partial Q}{\partial n} - Q\frac{\partial \theta}{\partial s} = 0, \tag{8}$$

in which case ϕ is defined by

$$\frac{\partial \phi}{\partial s} = Q, \qquad \frac{\partial \phi}{\partial n} = 0. \tag{9}$$

It is now necessary to solve the differential Eq. (8) along with Eq. (1) and (2). Using these, (8) may be written as a compatibility condition along the normal.

$$\frac{\partial Q}{\partial n} + \frac{Q}{\rho q^2}\frac{\partial p}{\partial n} = 0. \tag{10}$$

When computing the solution on a normal, the value of Q at the point D of definition of the normal must be chosen. A value which makes Q a continuous function is desirable; Q is defined to be αq on a streamline through D. The value of Q at the point of intersection of this streamline with a previously determined normal may be used to determine α.

If Q is continuous through vortex sheets and proportional to q through shocks then normals transform into lines $\phi =$ constant and the transformation is continuous.

3. Exceptional Lines and the Selection of Normals

Several types of discontinuities are of interest; discontinuities of derivatives on Mach lines and streamlines, shocks, and vortex sheets. It has also proved useful to keep track of certain Mach lines and streamlines across which no discontinuities occur. These will be referred to as *informational lines*. They are used to locate the points of formation of shocks in compression waves, to provide visual information in flow maps, and to preserve the accuracy of the computation. Informational Mach lines, sufficient in number to avoid a turning of the flow of magnitude greater than a specified $\Delta\theta_M$ between consecutive Mach lines of the same family, are introduced on the boundary streamlines and in point expansions. An informational streamline appears downstream of the intersection of an informational Mach line and a shock. The number of such streamlines is controlled by retaining one if the entropy change between it and another retained streamline exceeds a specified fraction of the total local entropy. All discontinuities and informational lines will be referred to as *exceptional lines.*

The intersections of exceptional Mach lines and streamlines—characteristics of the system of equations—present no difficulties beyond their location. No new discontinuities are generated at the points of intersection. When one shock or vortex sheet is involved, an intersecting discontinuity of derivative will be reflected and refracted. That is, a derivative discontinuity will appear on each streamline and/or Mach line or lines leaving the point of intersection. An exceptional line must be introduced. When two shocks or a shock and a vortex sheet intersect, one of the configurations (a), (b), or (c) in Fig. 1 may arise. The insertion of the necessary exceptional lines to represent the shocks and expansion waves is discussed further in Section 6 in a more general context which includes the possibility of multiple intersections and in which the case (d) in Fig. 1 may arise.

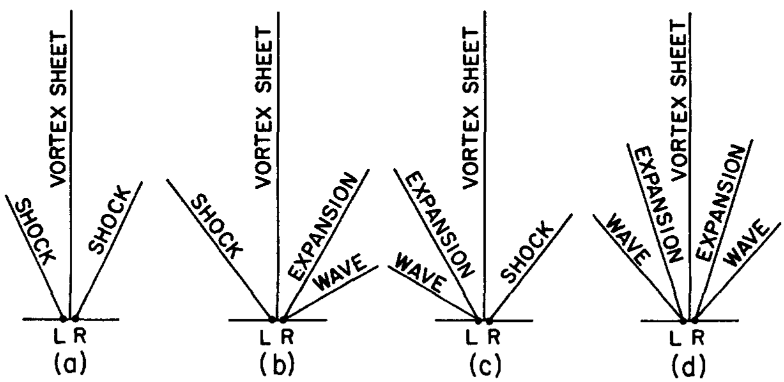

Fig. 1. Flows downstream of an intersection.

If flow variables are given at the limiting points L and R, identified in Fig. 1, the existence or nonexistence of a supersonic downstream solution must be determined and any solution found. Briefly, if $\theta = \Theta_R(p)$ is the inclination of flow, with pressure p, obtainable from flow at R, then Θ_R is derived from the Rankine–Hugoniot equations when $\hat{p}_R \geqslant p \geqslant p_R$ and from the isentropic flow relations when $p < p_R$. p_R is the specified pressure at R and $\hat{p}_R$ the maximum pressure obtainable by an oblique shock. A formal inverse function, $p = P_R(\theta)$, can be evaluated by Newton–Raphson iteration. Functions $\Theta_L(p)$ and $P_L(\theta)$ can be similarly defined. No supersonic solution exists if

$$\Theta_L(\hat{p}_L) > \Theta_R(\hat{p}_R)$$

or

$$P_L(\Theta_R(\hat{p}_R)) > \hat{p}_R$$

or

$$P_R(\Theta_L(\hat{p}_L)) > \hat{p}_L .$$

The solution, when it exists, can be found using "the rule of false position," (see [5]), applied to $F(p) \equiv \Theta_L(p) - \Theta_R(p) = 0$. This gives the algorithm

$$p^{(n+1)} = (p^{(0)}F(p^{(n)}) - p^{(n)}F(p^{(0)}))/(F(p^{(n)}) - F(p^{(0)})). \tag{11}$$

The values $\min(p_L, p_R)$ and $\min(\hat{p}_L, \hat{p}_R)$ for $p^{(0)}$ and $p^{(1)}$ insure linear convergence. When changes in $p^{(n)}$ for successive n are sufficiently small, the iteration is terminated and the associated value of θ obtained using $\theta = \Theta_R(p)$ or $\theta = \Theta_L(p)$. The obtained values of p and θ, (p^*, θ^*), appear on the vortex sheets in Fig. 1. The relationship of p^* to p_L and p_R indicates whether shocks or expansion waves are needed.

Considerable data manipulation may be necessary at intersections and it is not feasible to use a grid of equally spaced normals. In the procedure adopted a normal is generated through every intersection of exceptional lines and through every point on the boundary streamlines at which exceptional lines begin, that is at points of discontinuity and at selected points at which informational Mach lines are introduced.

The normals are constructed one at a time beginning at the inlet or upstream end of the duct and proceeding downstream. It may be that the normals selected by the criteria given above do not allow numerical integration of sufficient accuracy. In this case other normals are introduced. A step in ϕ, $\Delta\phi_M$, is defined as a function of a control parameter β and of the Mach numbers on the last known normal, $\phi = \phi_I$. If no intersection of exceptional lines occurs in the interval $(\phi_I, \phi_I + \Delta\phi_M)$ then the normal $\phi = \phi_I + \Delta\phi_M$ is generated. The parameter β is also used to determine the number of points at which the solution is found on each normal.

4. Numerical Techniques

If the Hartree [1] method is used to solve equations (1), (2), (3), and (10) with trapezoidal integration along characteristic segments and quadratic interpolation on normals then, if the third derivatives of the initial data are bounded, the numerical algorithms have error terms $O(\Delta^3)$ where Δ is a measure of the distance between selected normals and between points on those normals and $E(\Delta) = O(\Delta^3)$ means that there exist N and Δ^* such that $E < N\Delta^3$ for all $\Delta < \Delta^*$. Convergence of the method with error $O(\Delta^2)$ can be demonstrated by a modification of the methods used by Stetter [6] to study convergence of high accuracy algorithms on a mesh of two characteristics. The result is analogous to that of Courant, Isaacson and Rees [7] and holds when the Courant–Friedrichs–Lewy condition is satisfied. This condition, interpreted in the context of unequally spaced points on unequally spaced normals, is satisfied if every quadratic interpolation to determine values at a point X is based on a triad which spans X, that is, if no extrapolation occurs. A region of numerical dependence will then always span the corresponding region of analytic dependence. Further details appear in [5].

The algorithms used will be summarized. If an approximation $\mathbf{U}$ to the solution vector $\mathbf{u} = (q, p, \theta, Q)$ is known at points on $\phi = \phi_n$ and at W on $\phi = \phi_{n+1} = \phi_n + \Delta\phi_n$ then $\mathbf{U}$ may be found at a point P on $\phi = \phi_{n+1}$ by integration from W to P on $\phi = \phi_{n+1}$ and from $\phi = \phi_n$ to $\phi = \phi_{n+1}$ along the Mach lines and streamline through P. Figure 2 identifies the points P, W, L, C, and R.

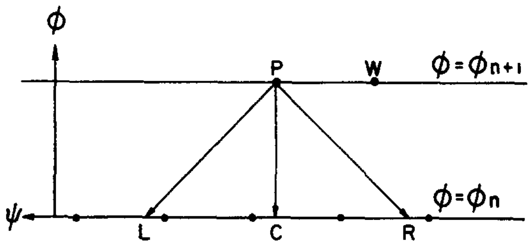

Fig. 2. The orientation of named points.

P is chosen so that $\psi_P - \psi_W = O(\Delta)$. The trapezoidal numerical integrals of (1) and (2) take the form

$$[(\rho q)_P + (\rho q)_C](q_P - q_C) + 2(p_P - p_C) = O(\Delta^3) \tag{12}$$

$$\pm [(\rho q^2)_P + (\rho q^2)_{\substack{R\\L}}](\theta_P - \theta_{\substack{R\\L}}) + [(M^2-1)_P^{1/2} + (M^2-1)_{\substack{R\\L}}^{1/2}](p_P - p_{\substack{R\\L}}) = O(\Delta^3). \tag{13}$$

Values at L, C, and R are obtained by quadratic interpolation on values at known parts on $\phi = \phi_n$. If these points are specified by their ψ coordinates, the values of ψ at L, C, and R are required; $\psi_C = \psi_P$, and

$$\psi_{\substack{R\\L}} = \psi_P \mp [g_P + g_{\substack{R\\L}}] \frac{\Delta\phi_n}{2} + O(\Delta^3) \tag{14}$$

where

$$g_P = \left(\frac{\rho q}{Q(M^2 - 1)^{1/2}}\right)_P, \text{ etc.,}$$

and

$$Q_P = \left[Q_W\left(2 - \frac{(p_P - p_W)}{(\rho q^2)_W}\right)\right]\left(2 + \frac{(p_P - p_W)}{(\rho q^2)_P}\right)^{-1} + O(\Delta^3). \tag{15}$$

The solution of Eqs. (12)–(15) may be derived iteratively. Initial values for the coefficients in square brackets in Eqs. (12)–(14) are necessary. Values for these terms at the point on $\phi = \phi_n$ nearest to ψ_C are suitable. Values of ψ_L and ψ_R are then obtainable from (14) and values of q_C, p_C, θ_R, θ_L, p_R, p_L can be obtained by interpolation. Solution of the now linear equations (12) and (13) yields an initial approximation $\mathbf{U}_P^{(0)}$, to the extended solution vector $\mathbf{u}_P = (q_P, p_P, \theta_P, Q_P, \psi_R, \psi_L)$.

An iterative solution of (14) was adopted rather than a direct solution of a quadratic equation for $\psi_{\substack{R\\L}}$. The computational simplicity of the direct solution is lost when R or L lies not on a normal but on a curved exceptional line (see Section 6).

Two approaches are now possible. The approximation $\mathbf{U}_P^{(r)}$ may be used to approximate the square brackets in both (12), (13), and (14) and then $\mathbf{U}_P^{(r+1)}$ may be obtained by solution of the linearized equations. Alternately, a two-stage method may be used in which the most recently obtained values are used in the coefficients, that is $\mathbf{U}_P^{(r)}$ is used to approximate the square brackets in (12) and (13) and $q_P^{(r+1)}$, $p_P^{(r+1)}$, $Q_P^{(r+1)}$, obtained when Eqs. (12) and (13) are solved, are used in (14). The convergence of both approaches for sufficiently small $\Delta\phi_n$ may be established by methods analogous to those used by Stetter [6].

The restriction of $\Delta\phi_n$ for both approaches is most significant immediately downstream of point expansions and immediately upstream of shock formation points in compression waves. The difficulty can be reduced by using a weighted combination of the two iterative schemes, the weights being dependent on the local derivatives of the Mach–line gradient. Details appear in [5].

The computation on exceptional Mach lines and streamlines can be achieved by a simple modification of the basic method. The value of ψ_L, ψ_C, or ψ_R becomes a known quantity and ψ_P must be determined. Vortex sheets present no difficulties.

Equation (12) is available on both sides of the discontinuity of q and ρ and the appropriate values must be used in the two forms of (13). The fitting of a shock is achieved by estimating ψ_P using an approximation to the angle of the shock. The flow upstream of the shock is then obtainable by the basic procedure described. A downstream flow with pressure p_1 and inclination θ_1 is defined by the shock angle approximation using the Rankine–Hugoniot equations. Application of the appropriate version of (13) downstream of the shock will yield a second downstream flow at P with inclination θ_1 but with a new pressure, p_2. The value $\frac{1}{2}(p_1 + p_2)$ is taken as the corrected downstream pressure at P and a new shock angle and hence gradient in (ϕ, ψ)-space is obtained using the Rankine–Hugoniot equations.

Two methods of defining boundary streamlines have been implemented. The first allows specification by a sequence of pairs $(\mathscr{F}_{B_i}, s_{B_i})$ where $\mathscr{F}_{B_i}$ is the value of a variable q, θ, p, M, or ρ at the point B_i with distance s_{B_i} along the streamline from the inlet of the duct. At a boundary point P only one compatibility relation on a Mach line is available. The relation required to complete definition of the solution at P is obtained by computing $\mathscr{F}_P$ using quadratic interpolation on the boundary data at three consecutive points $i = j, j + 1, j + 2$ chosen so that $s_{B_j} < s_P \leqslant s_{B_{j+2}}$. As the iteration to determine the solution at P proceeds, successive approximates to s_P are obtained using trapezoidal quadrature of Eq. (9) along the boundary streamline segment between $\phi = \phi_n$ and $\phi = \phi_{n+1}$.

The second method of defining the boundary streamlines specifies a focus point (X, Y) toward which or from which the boundary must direct reflected Mach lines. Geometrical considerations lead to a differential equation along such a boundary streamline.

$$\frac{1}{M[(X-x)^2 + (Y-y)^2]^{1/2}} = \frac{\gamma R T_0 M^2}{q^3(M^2-1)^{1/2}} \frac{\partial q}{\partial s} + \operatorname{sign}(\eta - \theta) \frac{\partial \theta}{\partial s}, \tag{16}$$

where η is the angle between the join of (X, Y) and (x, y) and the x-axis. A relation obtained by trapezoidal quadrature of this equation has been used successfully in place of the interpolation used in the first method.

5. Interpolation on Exceptional Lines

In the presence of discontinuities the iterative correction procedure described in Section 4 is inadequate. The Mach lines or streamlines through P may intersect an exceptional line between P and $\phi = \phi_n$. Values at this point of intersection must be found either by reapplication of the iterative procedure or by quadratic interpolation on the exceptional line. The latter course has been adopted as more feasible in regions containing a large number of exceptional lines. Figure 3 shows the points A, H, and B which are used to give values at L which lies on an exceptional line. The use of the point H on $\phi = \phi_{n+1/2} = \phi_n + \frac{1}{2}\Delta\phi_n$ is preferable to the use of the intersection of the exceptional line with $\phi = \phi_{n-1}$. This point may not exist, and even if it does, a gross disparity of $\Delta\phi_{n-1}$ and $\Delta\phi_n$ may lead to very poor interpolation. Values at L are obtained by interpolation with respect to ϕ, and ϕ_L

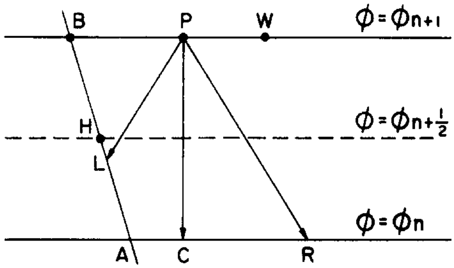

FIG. 3. Interpolation of an exceptional line.

must be determined taking into account the curvature of the exceptional line, that is by solving

$$\left.\begin{aligned}\psi_P - \psi_L + \tfrac{1}{2}[g_P + g_L](\phi_{n+1} - \phi_L) = 0\\ \psi_H - \psi_L - \tfrac{1}{2}[f_H + f_L](\phi_{n+1/2} - \phi_L) = 0\end{aligned}\right\} \tag{17}$$

where f is the gradient of the exceptional line. Since g_L and f_L are functions of ϕ_L the root nearest to $\phi_{n+1/2}$ of a cubic equation is needed. It is readily obtained by repeated approximation of the square brackets in (17), that is, using the iteration

$$\phi_L^{(s+1)} = \frac{2(\psi_P - \psi_H) + (g_P + g_L^{(s)})\,\phi_{n+1} + (f_H + f_L^{(s)})\,\phi_{n+1/2}}{(g_P + g_L^{(s)} + f_P + f_L^{(s)})}, \tag{18}$$

with $f_L^{(0)} = f_H$ and $g_L^{(0)} = g_H$. Similar formulas may be derived for the intersection of a streamline and Mach line of positive gradient with an exceptional line. The iteration (18) may proceed concurrently with that which determines $\mathbf{U}_P$.

Points on $\phi = \phi_{n+1/2}$ and exceptional lines cannot unfortunately be located unless the whole of the normal $\phi = \phi_{n+1/2}$ is found. It is convenient to determine $\phi = \phi_{n+1/2}$ at points having the same ordering and significance as the points used to determine $\phi = \phi_{n+1}$. The point storage on the normals is illustrated in Fig. 4. Each part of the strip between $\phi = \phi_n$ and $\phi = \phi_{n+1}$ which lies between two exceptional lines will be referred to as a block. Points at which the solution is determined on the new normals are marked $\times$. Interior exceptional lines are represented by pairs of points. In each block, interior points are assigned on the basis of a first approximation to the block length and the same number of interior points, equally spaced in ψ, are introduced on both $\phi = \phi_{n+1/2}$ and $\phi = \phi_{n+1}$.

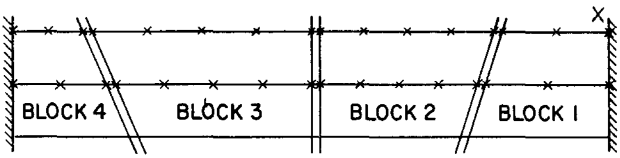

FIG. 4. Division of the calculation into Block calculations.

It must be noted that interpolation on the exceptional lines introduces a dependence of the solution which is foreign to the differential equations being solved. This makes it necessary to correct values at all points on the new normals 'together'. If the point X in Fig. 4 defines $\Delta\phi_n$ then construction and correction of the position and values on the normals must proceed to the left. If the exceptional line between blocks 1 and 2 is a Mach line then values in block 1 can be determined independently of the solution in other blocks but this is not true of blocks 2, 3, and 4 for which the dividing discontinuities lie respectively on a streamline and on a left-traveling Mach line or shock. The possibility of the solution at a point P depending on the solution at a point on the same normal further from X than P requires that point value corrections in each group of interdependent points be repeated sequentially, beginning with that point of the group nearest to X, until a repetition occurs in which at no point of the group are values significantly changed. The next group of interdependent points may then be considered. Pains must be taken to recognize the length of the groups so that excessive repetition of the point correction procedure is avoided.

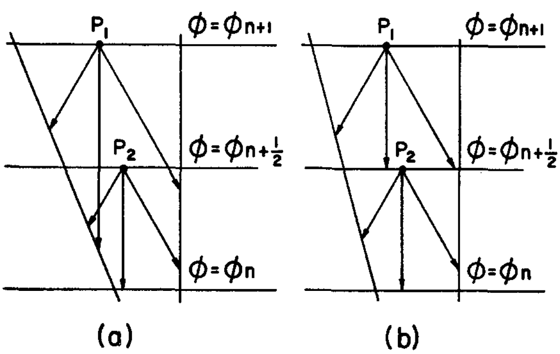

FIG. 5. Interpolation in (a) the initial and (b) the final stages of the iterative determination of the solution.

The use of the normal $\phi = \phi_{n+1/2}$ allows a development of the technique which makes the effective maximum ϕ step $\frac{1}{2}\Delta\phi_M$. If $\Delta\phi_n > \frac{1}{2}\Delta\phi_M$ then the calculation so far described and now represented for a block in Fig. 5(a) may be followed by the correction procedure represented in Fig. 5(b). The new correction uses interpolation on $\phi = \phi_{n+1/2}$ when applied to points on $\phi = \phi_{n+1}$. The points on $\phi = \phi_{n+1/2}$ must of course be further corrected because of their dependence on values at the intersections of $\phi = \phi_{n+1}$ with exceptional lines.

The nearest intersection of exceptional lines downstream of $\phi = \phi_n$ may not be found on the basis of a first order estimate and as the procedure progresses the need for informational Mach lines may be observed. Thus, the iterative procedure which determines values on the new normals must accomodate changes in the nature and point of definition of the normal $\phi = \phi_{n+1}$.

6. Data Manipulation

Discontinuities in the system described multiply very rapidly. To obtain an efficient procedure it is desirable to control the recognition of a discrete discontinuity. For example two vortex sheets which are sufficiently close together in some sense may be more quickly dealt with as a single vortex sheet. When an intersection of discontinuities occurs new discontinuities may be needed and these may remove the need to retain informational lines already in use. A systematic procedure is needed to represent the solution with the minimum number of exceptional lines necessary to provide required accuracy. A procedure has been written which attempts to do this.

As a first step all shocks and vortex sheets are examined and if they are sufficiently weak their status is lowered. They are treated as discontinuities of derivatives. Numerically obtained approximations to the values of derivatives of p, q, and θ are now compared on either side of each discontinuity of derivative. When the values differ by a quantity which could arise from the indeterminacy of the solution, the derivative discontinuities are ignored and the exceptional line involved becomes an informational line. The computation of the derivatives is carried out on the "half-way" normals $\phi = \phi_{n+1/2}$, etc., and, since no intersections occur on these, derivative estimates can always be made.

The second step involves removal and insertion of blocks and this is facilitated by generating lists of the blocks used in the solution and of available block names. Used and available points are similarly listed. The used-block list allows the block to the left or to the right of a given block to be found. The essential feature of the second step is the replacement of groups of blocks of short ψ-length by a minimal group bounded by divergent exceptional lines. If in a group of adjacent blocks each has ψ-length less than some chosen ϵ and if the most remote points of the group are less than 2ϵ distant then, if an intersection occurs between the exceptional lines which bound the blocks of the group, the group is replaced by one of the systems shown in Fig. 1, or by a simplification of one of these in which shock, vortex sheet or expansion wave is reduced in status to a derivative discontinuity, exceptional line, or simply omitted. The operation will deal with multiple intersections and will limit the density of intersections.

In the third step of the procedure any information lines which have been made superfluous by the presence of new discontinuities of derivative are removed. The fourth and final stage involves a search for steepening compression waves and the introduction of extra informational Mach lines to help locate incipient shocks.

7. Some Test Cases and Examples

The details of three calculations which demonstrate the accuracy of the method and of two calculations which demonstrate its diversity of application will be given. The computations were carried out on a Control Data 3600 computer and the flow maps appearing were produced on-line using a Data Display 80 film recorder.

The flow maps in Figs. 6–10 correspond to the five calculations to be described. In each map supersonic gas enters from the left. The maps are bounded at the top and bottom by boundary streamlines. Every second normal, the downstream member of every pair of calculated normals, is drawn and every exceptional line line is drawn. Shocks may be recognized visually by the bending of the normals which they cross.

Test 1. *Flow through a Focused Compression Wave*

This calculation tests several features of the program:

(a) the approximation of simple waves;

(b) the generation of a focusing surface using the method described at the end of Section 5;

(c) The positioning and simplification of a Mach-line focus.

The data given to the procedure appear in Table I which is included to exhibit some of the options available in the written program. The pressure, P_D, given on the inside boundary (see Table I) has been chosen to give a continuous transition from the wave to uniform flow beyond. Calculated values on informational Mach lines in the wave vary by less than 0.02 % and values at the downstream side of the wave are obtained with accuracy of 0.03 %. The focus is located with errors of

0.1 % in its coordinates. The computation required three minutes on the computer. This test is one of many which have been made using similar boundary conditions with different choices of P_D. If P_D is chosen to give a very weak shock then this

TABLE I

No.	Input Card Content
1	PLANE SUPERSONIC FLOW IN A DUCT. D. B. TAYLOR. CASE NUMBER 1
2	BEGIN FROM UNIFORM FLOW.
3	THE STAGNATION TEMPERATURE OF THE GAS, TO, IS 1452.4
4	THE RATIO OF SPECIFIC HEATS OF THE GAS, G, IS 1.4
5	THE UNIVERSAL GAS CONSTANT, GC, IS 1718.0
6	THE INITIAL FLOW HAS MACH NUMBER 3.0 AND THE DENSITY 0.002378
7	INSIDE DATA IN 2 BLOCKS BEGINNING AT X = 0.0, Y = 0.0
8	BLOCK 1 VALUES GIVEN AT 3 POINTS.
9	A DOWNSTREAM MACH-LINE FOCUS IS REQUIRED.
10	22.6274 AND 8.0 ARE THE X AND Y COORDINATES OF THE FOCAL POINT.
11	0.0 AND 20.0 ARE S AT THE START AND END OF THE BLOCK.
12	BLOCK 2 VALUES GIVEN AT 2 POINTS.
13	S PRESSURE
14	20.0 11454.4
15	40.0 11454.4
16	OUTSIDE DATA IN 1 BLOCK BEGINNING AT X = 0.0, Y = 16.0
17	BLOCK 1 VALUES GIVEN AT 2 POINTS.
18	S THETA
19	0.0 0.0
20	40.0 0.0
21	INTRODUCE AN INFORMATIONAL STREAMLINE AFTER EVERY 3.0 P.C. CHANGE IN ENTROPY.
22	INTRODUCE INFORMATIONAL MACH-LINES EVERY 2.0 DEGREES OF TURNING.
23	THE MINIMUM NUMBER OF SUBINTERVALS ON ANY NORMAL IS 10.
24	THE BASIC CONVERGENCE CRITERION PARAMETER IS 0.001
25	RETAIN THE RESULTS FOR DISPLAY.
26	TERMINATE THE CALCULATION ON THE NORMAL THROUGH THE POINT X = 45.0, Y = 15.0
27	DISPLAY WITH 6 UNITS OF LENGTH 2.0 PER FRAME.
28	PROVIDE DETAILED PRINTOUT AFTER NORMAL 1000.

must be located in the region of high derivatives which precedes the focus. The program has been written to achieve this by carefully measured underrelaxation in the iteration which determines the shock angle.

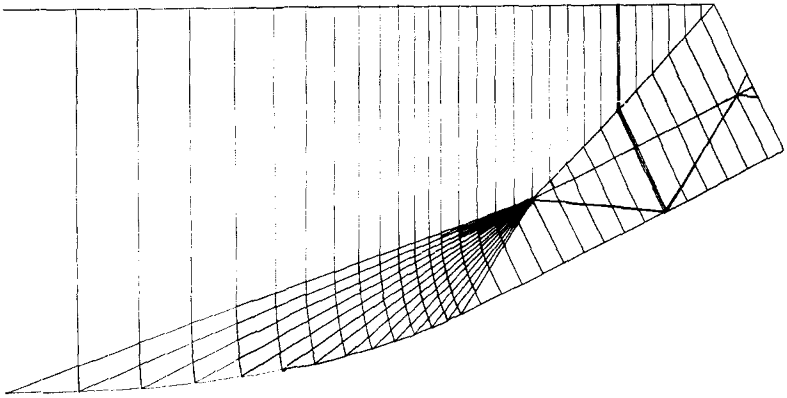

FIG. 6. Mach-3 flow through a focused compression wave, ($\gamma = 1.4$).

Test 2. *Flow between Wedges*

This tests the ability of the procedure to correctly manipulate shocks and their intersections. The test, one of several tests made, shows Mach-2 flow with $\gamma = 1.4$ between a 4° and an 8° wedge. The solution in this case is achieved throughout with errors of less than 0.1 %. The only errors arising from the solution of a differential equation originate in the weak expansion which is generated at the second intersection of discontinuities. Less than one minute of computation was required.

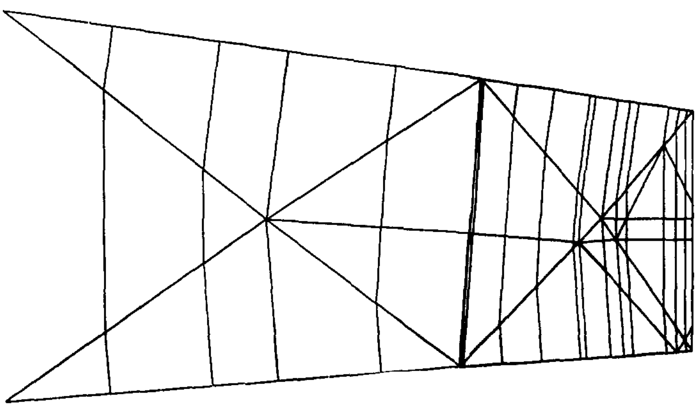

FIG. 7. Mach-2 flow between wedges, ($\gamma = 1.4$).

Test 3. *Expansion into a Region of Reduced Pressure*

This tests the introduction of expansions on boundaries and the implementation of the interaction of discontinuities with boundaries defined by pressure distributions. The data used specifies a flow with $M = 1.3$, $\gamma = 1.4$, entering a duct with $\theta = 0$ on one side and a constant value of pressure (0.767 of inlet pressure) on the other. Figure 8 shows a symmetric flow derived by reflection and addition from the calculated flow. The solution is almost periodic. The calculation did insert a shock and vortex sheet very close to the boundary at the focus points of the compression waves. The vortex sheets are just detectable in the figure by a thickening of the boundary streamlines downstream of the focus points. The computation required five minutes to give a solution which, by comparison with other tests, has errors of the order of 0.5 %.

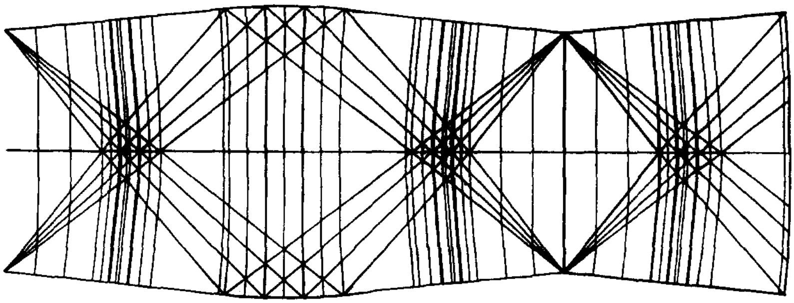

FIG. 8. Expansion into a region of reduced pressure ($M_\infty = 1.3$, $\gamma = 1.4$, $p_B/p_\infty = 0.767$).

Test 4. *Formation of a Shock from a Simple Wave*

The map shown in Fig. 9 shows Mach-3 flow incident on a wall composed of two circular arcs, the first concave and the second convex. The first arc has twice the

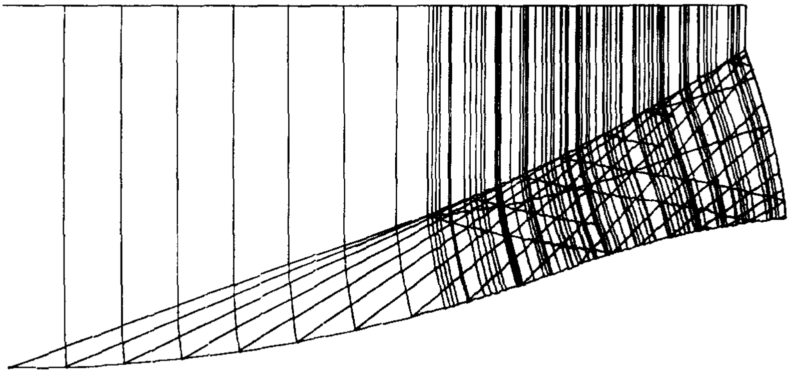

FIG. 9. Formation of a shock from a simple wave, ($M_\infty = 3$, $\gamma = 1.4$).

radius of curvature of the second. The first arc turns the flow through $+20°$ and the second, through $-20°$. Comparison with other tests using different step sizes indicates that errors are of the order of 1 %. The computation required 15 minutes.

Test 5. Flow around an Aerofoil

Figure 10 shows flow around an aerofoil defined by two circular arcs, both concave downwards, the upper arc turning the flow from 10° through 0° to −10° and the lower turning the flow from 5° through 0° to −5°. The problem was attacked as three duct problems:

(a) flow between the upper arc and a distant upper wall;

(b) flow between the lower arc and a distant lower wall;

(c) flow beyond the aerofoil, between distant walls.

The computations (a) and (b) provided data for (c). The three computations took 15 minutes in all.

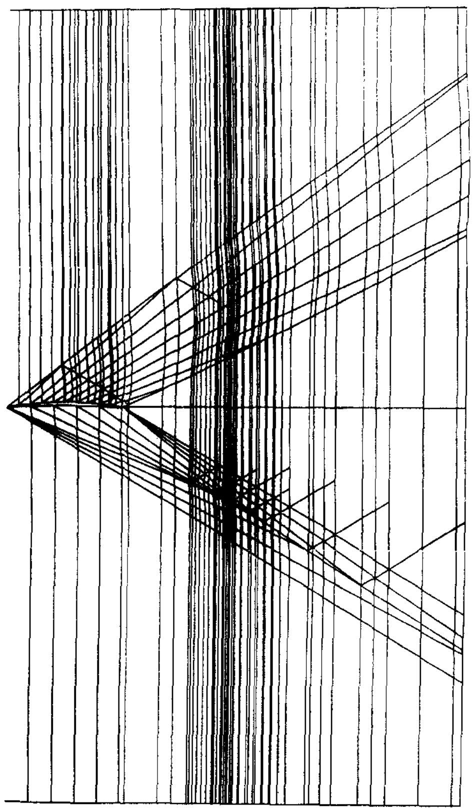

FIG. 10. Flow around an aerofoil ($M_\infty = 2$, $\gamma = 1.4$).

8. Conclusions

The methods developed give, at the cost of considerable programming complexity, highly accurate solutions, very rapidly—often more quickly than methods relying on artificial viscosity, see [8], for which Test 2 would not be an almost trivial calculation as it is here. A more detailed comparison with artificial viscosity methods would be interesting.

The author has recently completed the testing of a version of the procedure which will compute axially symmetric steady flows. The generalization of techniques using a discrete representation of discontinuities to three-dimensional and time dependent systems, while intriguing, represents a Herculean programming task which perforce subordinates this approach to methods employing artificial viscosity.

References

1. D. R. Hartree, Some Practical Methods of Using Characteristics In the Calculation of Non-steady Compressible Flow. USAEC Report AECU 2713 (1953).
2. A. I. Zhukov, Application of the Characteristics Method to the Numerical Solution of Unidimensional Problems in Gas Dynamics. *Isv. Akad. Nauk SSSR*, **1**, 149 (1960) and NASA Technical Translation F 298 (1967).
3. M. M. Moe and B. A. Troesch, *A.R.S.J.* **30**, 487–489 (1960).
4. S. A. Powers and J. B. O'Neill, *A.I.A.A. J.* **1**, 1693 (1963).
5. D. B. Taylor, The Calculation of Plane and Axisymmetric Steady Gas Flows Containing an Arbitrarily Large Number of Shocks. Argonne National Lab. Report. ANL 7491 (1968).
6. H. J. Stetter, *Num. Math.* **3**, 321–344 (1961).
7. R. Courant, E. Isaacson, and M. Rees, *Commun. Pure Appl. Math.* **5**, 243–255 (1952).
8. S. Z. Burstein, *J. Computational Phys.* **1**, 198–222 (1966).